MiR-199b-3p prevent the epithelial-mesenchymal transition (EMT) and fibrosis of renal tubule by regulating E-cadherin through targeting KDM6A in Diabetic nephropathy (DN)

Bo Tang
Department of Nephrology, Qingpu Branch of Zhongshan Hospital Affiliated to Fudan University
Weiliang Li
Departmen of Urology, Qingpu Branch of Zhongshan Hospital Affiliated to Fudan University
Tingting Ji
Department of Nephrology, Qingpu Branch of Zhongshan Hospital Affiliated to Fudan University
Xiaoying Li
Department of Nephrology, Qingpu Branch of Zhongshan Hospital Affiliated to Fudan University
Xiaolei Qu
Department of Nephrology, Qingpu Branch of Zhongshan Hospital Affiliated to Fudan University
Shoujun Bai (baishoujun@126.com)
Qingpu Branch of Zhongshan Hospital Affiliated to Fudan University https://orcid.org/0000-0002-3717-5053

Research

Keywords: Diabetic nephropathy, epithelial-mesenchymal transition, fibrosis, renal tubule, E-cadherin, KMD6A, miR-199b-3p, miRNA

Posted Date: May 13th, 2020

DOI: https://doi.org/10.21203/rs.3.rs-24819/v1

Abstract

Background

Diabetic nephropathy (DN) is the leading cause of end-stage renal disease. Although dysfunction of renal tubule, also exhibited as epithelial-mesenchymal transition (EMT) and fibrosis, is closely associated with DN, the mechanism underlying renal tubule dysfunction still remains obscure.

Methods

Here, we identify that miR-199b-3p protect renal tubule from diabetic- induced injury by repressing KDM6A, a histone lysine demethylase reinforcing diabetic renal tubule dysfunction through regulating E-cadherin expression. We investigated the relationship between KDM6A, E-cadherin and miR-199b-3p with a series of gain- and loss- function assay in different cell models and animal models. The expression of KDM6A, E-cadherin and miR-199b-3p was tested by qPCR, western bolt or IHC. The EMT was measured by wound healing assay. The dysfunction of renal tubule were observed through HE and PAS stain and the kidney functions were monitored through several pathological signs detection assay, such as albumin to creatinine ratio (ACR), blood urea nitrogen (BUN), creatinine (Cr), proteinuria.

Results

Lower expression of E-cadherin was related to a higher level of KDM6A, while E-cadherin was increased with KDM6A-inhibitor GSK-J4 treatment both in HG-induced HK-2 cells and STZ-induced kidney. However, the variable expression of E-cadherin caused by overexpression or silence RNA was failed to alter the KDM6A expression. The target prediction and dual-luciferase assay results showed miR-199b-3p is a new miRNA targeting KDM6A. Overexpression of miR-199b-3p increased E-cadherin expression and prevented EMT through repressing KDM6A expression in HG-induced HK-2 cells, whereas miR-199b-3p knockdown by inhibitor displayed opposite results with lower E-cadherin and worse EMT accompanying with higher level of KDM6A. In addition, the miR-199b-3p knockout mice exhibited more dysfunctional renal tubule and more serious damage in kidney tissue treated with STZ.

Conclusions

These results demonstrate that miR-199b-3p improve E-cadherin expression and prevent the progression of DN through targeting KDM6A. MiR-199b-3p could be a potential biomarker or target for the diagnosis and treatment of diabetic nephropathy in the future.

Introduction

Diabetic nephropathy (DN) is identified as the serious microvascular complication of diabetes which is one of the common causes of end-stage renal disease (1, 2). With an increasing number of new diagnoses and a 5-year survival rate of ~ 20%, DN has attracted much attention(3). A growing number of evidence elucidates the injury of proximal tubule critically helps to the renal injury and even the initial stage of DN(4). In recent years, many researchers have indicated that epithelial-mesenchymal transition (EMT), a main pathological process of renal tubular epithelial cell, promotes tubulointerstitial fibrosis which is the classical feature of end-stage renal disease including DN (5–8).

Most studies have focused on the role of TGF-β/BMP7/Smad pathways in the progression of DN, while recent studies indicate that chromatin modifications may also have a significant effect on the occurrence of DN(9–12). KDM6A (also

known as Histone demethylase UTX, ubiquitously transcribed tetratricopeptide repeat, X chromosome) was identified in 2007(13), which could specifically remove di- and tri- methyl groups from lysine 27 residue of histone H3 (H3K27) together with KDM6B (also known as JMJD3, jumonji domain containing 3) (14, 15). In this way, ectopic expression of KDM6A is closely associated with the changed gene expression. Interestingly, several reports have shown that KDM6A play a novel regulatory role in diabetic kidney disease. Chen H *et al* found KDM6A is in a position to regulate inflammation and DNA damage in db/db mice(16). Lin CL *et al* found that KDM6A can aggravate diabetic kidney injury through inducing podocytes dysfunction(17). However, little investigation has been done on expounding the role of KDM6A in renal tubulointerstitial fibrosis of DN.

MiRNAs are endogenous noncoding RNAs with 21–23 nucleotides (nt) which could regulate gene expression via binding to the 3'UTR of target gene mRNA(18). Recent advances in the study of miRNA have shown that miRNA can control the EMT and fibrosis in renal disease, indicating that miRNA may have a potent effect on DN. For example, miR-21, Let-7d miRNA, miR-302 showed an obvious activity to regulate the process of EMT and fibrosis in DN (19–21). We speculate that there is a miRNA participating in the progression of DN by targeting KDM6A mRNA.

In this study, we reported miR-199b-3p could alleviate the process of renal tubule EMT and fibrosis in DN though binding to KMD6A mRNA. We also explored the deleterious effect of KDM6A on aggravating the renal tubule injury via repressing E-cadherin expression.

Materials And Methods

Cell cultures, reagents and transfections

HK-2 cells obtained from China Center for Type Culture Collection (CCTCC) was cultured in MEM (5 mM D-glucose) (Gbico) supplemented with 10% FBS (Gbico), 100ug/ml streptomycin and 100 U/ml penicillin (Hyclone) at 37 °C with 5% CO2. For EMT induction, HK-2 cells were growth in high glucose medium (30 mM D-glucose) or high mannitol medium (5 mM D-glucose and 25 mM mannitol) for 72 h. All primary antibodies were purchased from Abcam and all second antibodies were obtained from Sino Biological. Streptozotocin (STZ) and GSK-J4 were obtained from sigma.

For HK2-E-cadherin stable cell line, HK-2 cells were infected with lentivirus contain E-cadherin encoding sequence or not and selected with puromycin (sigma, 2ug/ml) for 2 weeks. The package of lentivirus was performed in HEK293T co-transfected with psPAX2, pMD2G and pCDH-CMV-Mcs-Ef1-Puro (Addgene) for 72 h. For HK2-miR stable cells, HK-2 cells were infected with lentivirus contain miR-199b-3p or miNC as described(22). The silence RNA for negative control (si-NC), silence RNA for downregulating E-cadherin (si-E-cadherin) were obtained from Invitrogen. The miR-199b-3p inhibitor (inhibitor) and inhibitor NC were obtained from RiboBio.

Transfection experiments were performed by using Lipofectamine 2000 reagent according to the manufacturer's instruction (Thermo Fisher Scientific).

The sequence of siRNA and miRNA was exhibited in Table S2.

Wound Healing Assay

The cells were seed at the density of 5×10^5 cells/well in 6-well plates. The cell monolayer was performed by a 200μL pipette tip for forming "wound". Photographs were taken after 0 h and 48 h. The wound areas were measures by ImageJ software and the "relative wound area" was normalized by wound areas at 0 h.

Animals, Diabetic Animal Models And GSK-J4 Treatment

Male C57BL/6 mice (Guangdong Medical Laboratory Animal Center) were intraperitoneally given 190 mg/kg STZ or equivalently normal saline to induce diabetes. The blood glucose levels were equalized by adding 1–2 unit/kg insulin in each diabetic mouse as decreased previously[17]. Mice were seen as diabetes with 200–300 mg/dl of fasting blood glucose. For GSK-J4 treatment, mice were subcutaneously injected with 0.4 mg/kg each day at 1 week after onset of diabetes. MiR-199b-3p knockout mice were obtained from C57BL/6 mice through Nanjing Biomedical Research Institute of Nanjing University.

Mouse Metabolic Measurements

Albuminuria of was quantified by albumin and creatinine ratio (ACR) with mouse albumin ELISA kit (Bethyl Laboratories). Creatinine was detected through the Creatinine Assay Kit (BioAssay System). BUN was tested by Urea Assay Kit (BioAssay System). Proteinuria was examined by Proteinuria Elisa kit (Nanjing Anyan Biological Technology). All of those assays were performed at 8 weeks after the onset of diabetes in each mice.

Quantitative Real-time PCR

Total RNA was extracted using the Trizol reagent (Invitrogen) and cDNAs were gained using PrimeScript RT reagent kit (TaKaRa) except that of miRNA by TaqMan Advanced miRNA cDNA synthesis kit (Waltham). PCR quantification was performed as previously decreased(23). To test the expression of miRNA, we used stem-loop qRT-PCR for miR-199a-3p, miR-199b-3p and miR-758-3p following the protocol decreased previously(24, 25). Primers was showed in Table S2.

Protein Extraction And Western Blot Analysis

Proteins were extracted from cells and mice kidney (Beyotime Biotechnology) and the protein lysates (20 μg) were quantified through bicinochoninic acid assay kit (BOSTER). Then the proteins of each sample were loaded in lane and tested in SDS-PAGE gel at 80V for 30 min and then 100V for 1 h after boiling for 5 min at 100 °C in loading buffer. Next, the proteins were transferred to a nitrocellulose membrane (Boster) at 300A for 1.5 h. The membranes were blocked in Tris-buffered saline contain 0.1% Tween 20 (TBST) and 5% fat-free milk for 1 h. Then the membranes were incubated with first antibodies overnight at 4 °C. After washing, the membranes were incubated with second antibodies for 2 h at room temperature. The membranes were treated with high-sig electrochemiluminescence kit (Fdbio Science) and detected by an image analysis system (Image-Pro Plus 6.0, Media Cybernetics).

Dual Luciferase Assay

HEK293T cells were transfected with pMIR-KDM6A 3'-UTR, pMIR- KDM6A 3'-UTR mutant plasmid (500 ng) accompanied with pRL-TK plasmid (50 ng) (Promega), respectively. At the same time, miR-199b-3p mimics or negative control (150 nM) was co-transfected with those plasmids. Luciferase activity was examined using Dual Luciferase Reporter Assay System (Promega) at 48 h after transfection(26).

Tissue Histochemical Staining, HE And PAS Staning

Mouse kidneys were obtained in separate treated mice at 8 weeks after the onset of diabetes. Mouse kidneys embedded in paraffin were cut into 4-mm-thick sections and stained with PAS and HE (Sigma). Stained slides were observed by an experienced pathologist for histopathological examination under light microscopy. For histochemical staining, paraffin-embedded sections were stained with anti-KDM6A, anti-E-cadherin and anti-TGFβ as described previously(27).

Statistical analysis

Data in the study were analyzed by using Prism (version 5; GraphPad Software) and were compared through the Student's t test. It expressed as the Mean ± SD. Values were considered statistically significant if $P < 0.05$.

Results

KDM6A showed a promotive activity for regulating the EMT in HK-2 cells

Bearing in mind the importance of epigenetic modification in the development of kidney disease, we firstly investigated the expression and significance of KDM6A in the HK-2 cells cultured in high glucose (HG) and mannitol (Mann) medium. First of all, we confirmed the change of HK-2 migration in the HG group, which is closely associated with epithelial-mesenchymal transition(28), HG-induced HK-2 cells showed a significant deteriorative migration relative to Mann groups, suggesting HK-2 cells displayed severe epithelial-mesenchymal transition when cultured in HG medium(Fig. 1A). The EMT maker, E-cadherin and TGFβ, were detected by immunoblotting and qPCR. The immunoblotting results showed an increased tendency of E-cadherin and TGFβ expression in HG-induced HK-2 cells comparing to Mann-induced group (Fig. 1B), consistent with the qPCR results (Fig. 1C). Interestingly, the expression of KDM6A in the HG group was also elevated both in transcription and translation level (Fig. 1B-C), indicating that upregulation of KDM6A may be associated with the EMT progress of HK-2 cell induced by HG.

To confirm the hypothesis, GSK-J4, a kind of KDM6A inhibitor, was utilized to treat HK-2 cells in HG medium with negative control (NC and GSK-J4). The migration detected by wound healing assay was decreased while the HK-2 cells were treated with GSK-J4 (Fig. D). The lower expression of E-cadherin and TGFβ was observed by western bolt and qPCR in the GSK-J4 groups, expounding the inhibition of KDM6A could receded the EMT degree in HG-induced HK-2 (Fig. E, F).

Those results illustrated that KDM6A might be able to propel the progression of epithelial-mesenchymal transition in renal tubular epithelial cells.

KDM6A exhibited a pivotal role in kidney injury of DN

Basing on the *in vitro* studies, we next investigated the *in vivo* role of KDM6A in diabetes kidney of DN using a STZ-induced mouse model (WT-NC groups and WT-STZ groups). We indeed found a higher level of KDM6A was expressed in kidney tissues of the 12-week STZ-induced diabetic mice relative to control groups, both measured by qPCR and Immunohistochemistry (IHC) (Fig. 2A-C). To further explore the influence of KDM6A on the progression of diabetes kidney injury, GSK-J4 was applied to treat diabetic mice with negative control (WT-STZ-NC and WT-STZ-G groups). The injury of diabetic kidney was evaluated through the morphology of renal proximal tubule and renal distal tubule which were associated with tubulointerstitial fibrosis. Obviously, the HE and PAS stain results in kidney of STZ-induced mice showed renal proximal tubular epithelial cells expansion and proximal tubule lumen reduction relative to normal mice, while the degree of proximal tubule injury in diabetic mice was dramatically decreased after treated with GKS-J4 (Fig. 2D, F). Similarly, severe fibrosis of renal distal tubule in diabetic mice was monitored and the progress of fibrosis was retarded in the presence of GKS-J4 (Fig. 2E, G). In those GSK-J4-induced or non-GSK-J4-induced diabetic mice, several typical signs of diabetic nephropathy, such as albumin to creatinine ratio (ACR), blood urea nitrogen (BUN), creatinine (Cr), proteinuria,

was measured. All of those sighs were aggravated in STZ-induced mice and restored partly by GSK-J4 treatment (Fig. 2H-K), which were closely consistent with HE and PAS stain results. Those results indicated that the downregulation of KMD6A might alleviate the kidney injury of diabetic nephropathy mice.

Interestingly, the IHC and its quantitative results displayed a suppressed expression of E-cadherin, a maker of EMT and fibrosis process(14), and an elevated expression of TGF-β, another maker of EMT and fibrosis process(6), whereas both of them were altered by GSK-J4 (Fig. 2L-O). Treated diabetic mice with GSK-J4, the depressed E-cadherin was recovered and the increased TGF-β was downregulated, totally conforming to the previous results.

Together, the expression of KDM6A was improved in the kidney tissues of STZ-induced diabetic nephropathy mice and the inhibition of KDM6A resulted in a mitigative kidney injury, suggesting that KDM6A could promote the progress of diabetic nephropathy.

KDM6A was the upstream regulator of E-cadherin for repressing the its expression

Tons of reports have showed that repressing the epithelial cadherin (E-cadherin) could trigger the EMT and fibrosis directly (29, 30). Depending on the previous work, we assumed that KDM6A might be the upstream effector of E-cadherin and could inhibit the E-cadherin expression, resulting in EMT and even fibrosis of DN. To testify our assumption, HK-2 cells stably overexpressed E-cadherin (HK2-vehicle and HK2-E-cadherin groups) was constructed. Overexpressing E-cadherin could inhibit the EMT process and reduced the migration of HK-2 cells comparing to HK2-vehicle groups when cells were cultured in HG medium (Fig. 3A). However, as the increasing of E-cadherin in HK2-E-cadherin groups, the expression of KDM6A showed no difference in both transcription and translation level between HK2-vehicle and HK2-E-cadherin groups (Fig. 3B, C). It seemed that KDM6A expression might be not affected by overexpressing E-cadherin.

Furthermore, the silencing RNA, targeting E-cadherin (si-E-cadherin), was applied to knockdown the E-cadherin in HK-2 cells as well as negative control (si-NC) when cells were cultured in mannitol medium. In this condition, the migration of HK-2 was improved dramatically with the E-cadherin knockdown (Fig. 3D). Notably, the expression of KDM6A was either still in a stable state even if the EMT was aggravated by E-cadherin knockdown (Fig. 3E, F). All those results showed the expression of KDM6A would not be impacted only by variation of E-cadherin expression, suggesting that KDM6A was the upstream regulator of E-cadherin.

KDM6A was the target of miR-199b-3p during the renal injury

Considering the importance of miRNA in development of diabetic nephropathy, we wanted to determine whether miRNA participated in the progression of DN by targeting KDM6A mRNA. For mining potential miRNA candidates targeting KDM6A, we predicted possible miRNA by several databases, such as PITA, RNA22, miRmap, microT, miRanda, PicTar, and TargetScan, Finally, we found 8 miRNAs, hsa-miR-19a-3p, hsa-miR-19b-3p, hsa-miR-23a-3p, hsa-miR-199a-3p, hsa-miR-23b-3p, hsa-miR-199b-3p, hsa-miR-758-3p, hsa-miR-142-3p. Each of miRNAs were exhibited from at least 5 databases (Table 1). Among of them, hsa-miR-142-3p, hsa-miR-19a-3p, hsa-miR-19b-3p, hsa-miR-23a-3p and hsa-miR-23b-3p have been proved for binding to *KDM6A* in kidney (26, 31–33). Additionally, the fold-change of hsa-miR-199a-3p, hsa-miR-199b-3p, hsa-miR-758-3p between normal kidney and kidney with DN was analyzed by GEO DataSets. The results of GSE51674, a dataset acquired from the progression of kidney fibrosis in human Diabetic Nephropathy, showed noticeable change of hsa-miR-199a-3p, hsa-miR-199b-3p expression, but no difference in hsa-miR-758-3p expression (Fig. S1A, B, Table S1). The change of hsa-miR-199b-3p expression was remarkably outstanding compared with other 2 miRNAs.

Table 1
The predictive results of miRNA targeting KDM6A

miRNA ID	miRNA name	Databeses							Numbers of datebase
		PITA	RNA22	miRmap	microT	miRanda	PicTar	TargetScan	
MIMAT0000073	hsa-miR-19a-3p	√	×	×	√	√	√	√	5
MIMAT0000074	hsa-miR-19b-3p	√	×	×	√	√	√	√	5
MIMAT0000078	hsa-miR-23a-3p	√	×	×	√	√	√	√	5
MIMAT0000232	hsa-miR-199a-3p	√	×	√	√	×	√	√	5
MIMAT0000418	hsa-miR-23b-3p	√	×	×	√	√	√	√	5
MIMAT0000434	hsa-miR-142-3p	√	×	√	√	√	√	√	6
MIMAT0003879	hsa-miR-758-3p	√	×	√	√	√	√	√	6
MIMAT0004563	hsa-miR-199b-3p	√	×	√	√	×	√	√	5

To confirm the results, qPCR assay was performed for testing those miRNA expression in HG-induced HK-2 cells and the results showed a similar trend with precious work (Fig. 4A). We also detected the miRNA expression in diabetes kidney using a STZ-induced mouse model. The results was compatible with the consequence in HG-treated HK-2 cell (Fig. 4B).

Considering the greatest change of miR-199b-3p, we assumed that miR-199b-3p could bind to KDM6A mRNA. According to the predicted alignment of miR-199b-3p binding to KDM6A mRNA (Fig. 4C), WT and mutant KDM6A 3'UTR luciferase plasmids as well as miR-199b-3p mimics and mi-NC were designed for dual-luciferase reporter assay in order to confirm the prediction. Comparing with cells co-transfected with WT KDM6A 3'UTR and mi-NC, cells co-transfected with WT KDM6A 3'UTR and miR-199b-3p mimics displayed a conspicuous reduction of luciferase activity. However, when the WT KDM6A 3'UTR was replaced by mutant KDM6A 3'UTR, no luciferase activity change could be observed regardless of co-transfecting with miR-199b-3p mimics or mi-NC (Fig. D).

Those results suggested that miR-199b-3p expression was changed in the EMT of renal tubular epithelial cells and could target to *KDM6A*, which means miR-199b-3p may play a regulatory role in tubulointerstitial fibrosis of DN through downregulate KDM6A.

MiR-199b-3p showed a protective effect against epithelial-mesenchymal transition of renal tubular epithelial cells through downregulating KDM6A

For further explore the role of miR-199b-3p in the process of EMT in renal tubular epithelial cells, we transfected the HK-2 cells with lentivirus containing miR-199b-3p mimics or miR-NC and selected the stable cell line (HK2-miRNA and HK2-miNC) and cultured them in HG medium. The expression of miR-199b-3p in both cell lines was tested (Fig. S2A). As the increasing expression of miR-199b-3p in HK2-miRNA, the expression of KDM6A, measured by western blot, was inhibited in HK2-miRNA cells (Fig. 5A) with a slightly lower transcription level of KDM6A detected by the qPCR (Fig. S2A). The expression of TGFβ and E-cadherin was also tested. Decreased expression of TGFβ was observed, whereas the expression of E-cadherin was upregulated relative to HK2-miNC cells (Fig. 5A). The similar tendency was also monitored in transcription level (Fig. S2B). Furthermore, the HK2-miNC cells in HG showed a more serious EMT than HK2-miRNA cells in HG with the deteriorative migration, suggesting that miR-199b-3p could halt HG-induce EMT of HK-2 cells dramatically (Fig. 5B). Those results indicated that miR-199b-3p might be able to downregulate the KDM6A and further protected HK-2 cell from the HG-induced injury.

In order to confirm the influence of miR-199b-3p on HK-2 cells through downregulating KDM6A, we transfected HK2-miRNA cells with a miR-199b-3p inhibitor (inhibitor) or negative control (inhibitor NC) to determine whether inhibition of miR-199b-3p could exacerbate HG-induced EMT. The qPCR results showed the successful inhibition of miR-199b-3p because of the inhibitor, accompanying with the restored expression of KDM6A (Fig S2. C). Consistently, the maker of EMT, TGFβ and E-cadherin, showed an increased and decreased tendency respectively, no matter in mRNA level or protein level (Fig. 5F, Fig. S2D). As we supposed, the expression of KDM6A in translation level was certainly restored due to the inhibitor existence (Fig. 5C). In the presence of inhibitor, migration of HK2-miRNA cells were increased, which indicated HK2-miRNA cells were preferred to mesenchymal-like performance compared with inhibitor NC group (Fig. 5D). Those results suggested that the restoration of KDM6A due to repression of miR-199b-3p could aggravate the EMT process.

Together, miR-199b-3p could prevent the degeneration of EMT in renal tubular epithelial cells through suppressing KDM6A expression.

MiR-199b-3p could inhibit the kidney injury caused by diabetic nephropathy by regulating KDM6A expression

In order to further confirm the function of miR-199b-3p *in vivo*, we induced the diabetic nephropathy in miR-199b-3p deficient mice (miR-199b-3p$^{-/-}$, Fig. S3A) using STZ as well as negative control (miR-199b-3p$^{-/-}$-NC and miR-199b-3p$^{-/-}$-STZ). Several typical signs of DN were measured in different groups and all of them showed a similar tendency. The level of ACR, BUN, Cr and proteinuria in miR-199b-3p$^{-/-}$-STZ groups were significantly greater than WT-STZ groups, indicating the protective function was removed due to the miR-199b-3p deficiency (Fig. 6A-D). Furthermore, the pathological features of STZ-induced diabetic kidney in WT and miR-199b-3p$^{-/-}$ mice were observed through HE and PAS stain. Also in the induction of STZ, a more serious renal proximal tubular epithelial cells expansion as well as a more severe proximal tubule lumen reduction was emerged in miR-199b-3p$^{-/-}$ mouse compared to WT mouse (Fig. 6E, G). Consistently, more severe fibrosis of renal distal tubule was monitored due to the miR-199b-3p deficiency (Fig. 6F, H). Comparing with WT-STZ groups, the IHC and qPCR results in miR-199b-3p$^{-/-}$-STZ groups showed an increased expression of TGFβ and a decreased expression of E-cadherin, which was consistent with pathological results (Fig. 6I-J, L-M, Fig. S4B). However, the higher level of KDM6A was expressed in diabetic kidney tissues without miR-199b-3p existence, no matter in transcription or translation level (Fig. 6K, N, Fig. S4B).

Summarily, based on those *in vivo* results, we evidently found the absence of miR-199b-3p was closely associated with the exacerbation of kidney injury in STZ-induced diabetic mice by abolishing the repression of KDM6A, indicating that miR-199b-3p played a protective prole in kidney injury of diabetic nephropathy through downregulating KDM6A.

Discussion

Despite numerous studies, the therapeutic interventions in preventing diabetes nephropathy are still not enough, which means more potential pathways for participating in the progression of diabetes nephropathy have yet to be explored. Here, our study demonstrates that the upregulation of KDM6A in diabetic kidney can inhibit the E-cadherin expression and trigger the epithelial-mesenchymal transition and fibrosis of renal tubular epithelial cell in diabetic kidney and eventually lead to diabetes nephropathy. However, we find a new role of miR-199b-3p in DN, which exhibit the characteristic of protecting the kidney from diabetic-induced injury by repressing the KMD6A expression.

Many studies have suggested that epithelial-mesenchymal transition plays an important role in renal fibrosis which is a pathological feature of kidney disease containing diabetic nephropathy (5–8). In the present work, we found that KDM6A could promote the progression of EMT in HK-2 cells induced by HG. Similarly, a positive role of KMD6A in regulating the migration and invasion of hematopoietic stem cells and breast cancer cells, usually caused by EMT, indicated that KMD6A might positively regulate the EMT in those cell types(34, 35). Our results from in vivo experiments expounded that the inhibition of KDM6A could decrease the degree of EMT and fibrosis of diabetic kidney and ease the symptoms of kidney injury. Coincidentally, Lin CL *et al* also found the suppression of KDM6A in STZ-induced mice showed a protective role in kidney injury. They further demonstrated that KDM6A aggravate DN through disturbing podocyte function by increasing KLF10 which could inhibit nephrin expression(17). Chen H et al showed that overexpression of KDM6A accelerated the progression of diabetic kidney diseases(16). Furthermore, we found that the expression of E-cadherin, a key regulative gene of EMT, would decrease with the increased of KDM6A, whereas KDM6A expression was not affected by the change of E-cadherin expression, indicating that E-cadherin might be the downstream target of KDM6A. However, the role of KDM5A in EMT progression remains controversial. Van den Beucken *et al* showed that inhibition of KDM6A promote EMT and cancer stemness (36) and Zhou Z *et al* showed that downregulation of KDM6A repressed the E-cadherin expression (37), which could be attributed to increasing histone H3K27 methylation. Considering multiple performance of KDM6A during EMT in different diseases or cell types, KDM6A may regulate the EMT process in many different pathways. According to that, we hypothesize that other transcription factors might be existed which improve the E-cadherin expression and was repressed by KDM6A. To confirm the hypothesis, more investigation needs to be done in the further.

Many studies showed that miR-199b-3p was expressed in many kinds of tissue and most of them displayed a functional role in different cancer. Graham ME et al showed miR-199b-3p in the serum of patients with papillary thyroid cancer was downregulated dramatically(38). Wang X et al found miR-199b-3p was one of the key miRNA related to hepatocellular carcinoma(39). Koshizuka K et al showed that miR-199b-3p inhibited cancer cell migration and invasion in head and neck cancer by regulating ITGA3(23). Similarly, Sakaguchi T et al also found miR-199b-3p functioned as a tumour suppressor in bladder cancer by targeting ITGA3(40). In addition to cancer, miR-199b-3p also play an important role in other disease. The apoptosis of cerebral microvascular endothelial cells was repressed via upregulation of miR-199b-3p in ischemic stroke(25). Wu G et al showed miR-199b-3p was substantially increased in extracellular vesicles from nasal mucus from patients with Allergic Rhinitis(41). Dolz S et al also found miR-199b-3p presented remarkablely higher expression in patients with asymptomatic carotid artery stenosis progression(42). However, the role of miR-199b-3p on diabetic nephropathy is unclear. As described in this study, KDM6A has been reported to be regulated by several miRNAs in kidney tissue. We, for the first time, defined KDM6A as a target of miR-199b-3p in diabetic kidney, which may provide new insights into the mechanisms of diabetic nephropathy progression. Although miR-199b-3p was proved to relieve the diabetes-induced kidney injury through inhibiting KDM6A expression here, its upregulation was observed in HG-induced HK-2 cell and kidney tissues of STZ-induced mice, which might be explained by the compensation for the higher expression of KDM6A.

Conclusion

We here provide evidence that KDM6A promotes the epithelial-mesenchymal translation and fibrosis of renal tubular epithelial cells in kidney of diabetic nephropathy through downregulating the expression of E-cadherin and eventually results in severe kidney injury, while miR-199b-3p rescues the renal damage by repressing KDM6A expression. In the future, miR-199b-3p may be a potential biomarker or target for the diagnosis and treatment for diabetic nephropathy.

Abbreviations

DN, Diabetic Nephropathy; EMT, Epithelial-Mesenchymal Transition; STZ, Streptozotocin; HG, high glucose; Mann, mannitol; IHC, Immunohistochemistry; ACR, Albumin to Creatinine Ratio; BUN, Blood Urea Nitrogen; Cr, creatinine.

Declarations

Ethical Approval and Consent to participate

Not applicable

Consent for publication

Not applicable

Competing interests

None of the authors have any competing interests in the manuscript.

Funding

This work was supported by the Fund of Shanghai Municipal Commission of Health and Family Planning (201840254).

Authors' contributions

BT designed this study. SB supervised the study. BT, WL, TJ, XL and XQ contributed to experiments and data analysis. BT and WL prepared the manuscript and SB revised the manuscript. All authors read and approved the final manuscript. Thank you for other support from colleagues of Qingpu Branch of Zhongshan Hospital Affiliated to Fudan University.

Acknowledgements

This work was supported by the Fund of Shanghai Municipal Commission of Health and Family Planning (201840254).

Availability of data and materials

The datasets used and/or analyzed in the current study are available from the corresponding author on reasonable request. The datas about GEO analysis is public data in dataset GSE51674 in GEO DataSets.

References

1. AJ C, RN F, B C, D G, C H, A I, et al. US Renal Data System 2013 Annual Data Report. American journal of kidney diseases : the official journal of the National Kidney Foundation. 2014;63:A7.
2. SS B, FR D. New insights into molecular mechanisms of diabetic kidney disease. American journal of kidney diseases : the official journal of the National Kidney Foundation. 2014;63:S63-83.
3. C M, DJ G, CJ W, DP B. Diabetic Nephropathy: a Tangled Web to Unweave. Cardiovascular drugs and therapy. 2017;31:579-92.

4. K H, S W, P S, Y S, H M, K F, et al. Renal tubular Sirt1 attenuates diabetic albuminuria by epigenetically suppressing Claudin-1 overexpression in podocytes. Nature medicine. 2013;19(11):1496-504.
5. F W, S E, GD K, A Z, G D, H M, et al. Diabetic nephropathy and hypertension in diabetes patients of sub-Saharan countries: a systematic review and meta-analysis. BMC research notes. 2018;11(1):565.
6. L Z, G J, X H, Q Y, Z S. The inhibition of SGK1 suppresses epithelial-mesenchymal transition and promotes renal tubular epithelial cell autophagy in diabetic nephropathy. American journal of translational research. 2019;11(8):4946-56.
7. Z Z, M G, Y J, D W, R P, F L, et al. The coordinated roles of miR-26a and miR-30c in regulating TGFβ1-induced epithelial-to-mesenchymal transition in diabetic nephropathy. Scientific reports. 2016;6:37492.
8. Y J, Z Z, Y Y, M Z, J L, L W, et al. MiR-4756 promotes albumin-induced renal tubular epithelial cell epithelial-to-mesenchymal transition and endoplasmic reticulum stress via targeting Sestrin2. Journal of cellular physiology. 2019;234(3):2905-15.
9. R K, D M, O D, B X, TT O, K B. Epigenetic changes in renal genes dysregulated in mouse and rat models of type 1 diabetes. Laboratory investigation; a journal of technical methods and pathology. 2013;93(5):543-52.
10. D F. Epigenetic control of podocyte differentiation: a new target of the renin-angiotensin system in kidney disease. Kidney international. 2015;88(4):668-70.
11. S M, A A. The epigenetic regulation of podocyte function in diabetes. Journal of diabetes and its complications. 2015;29(8):1337-44.
12. XM M, AC C, HY L. Role of the TGF-β/BMP-7/Smad pathways in renal diseases. Clinical science (London, England : 1979). 2013;124(4):243-54.
13. S H, YW C, LR Y, H Y, TD V, K G. Identification of JmjC domain-containing UTX and JMJD3 as histone H3 lysine 27 demethylases. Proceedings of the National Academy of Sciences of the United States of America. 2007;104(47):18439-44.
14. HJ C, JH P, M P, HY W, HS J, CH L, et al. UTX inhibits EMT-induced breast CSC properties by epigenetic repression of EMT genes in cooperation with LSD1 and HDAC1. EMBO reports. 2015;16(10):1288-98.
15. K A, PA C, J C, D P, S R, J R, et al. UTX and JMJD3 are histone H3K27 demethylases involved in HOX gene regulation and development. Nature. 2007;449(7163):731-4.
16. H C, Y H, X Z, C L, Y Y, H S, et al. Histone demethylase UTX is a therapeutic target for diabetic kidney disease. The Journal of physiology. 2019;597(6):1643-60.
17. CL L, YC H, YT H, YH S, CJ W, WC C, et al. A KDM6A-KLF10 reinforcing feedback mechanism aggravates diabetic podocyte dysfunction. EMBO molecular medicine. 2019;11(5).
18. DP B. MicroRNAs: genomics, biogenesis, mechanism, and function. Cell. 2004;116(2):281-97.
19. L L, Y W, R Y, L L, X Z, H L, et al. BMP-7 inhibits renal fibrosis in diabetic nephropathy via miR-21 downregulation. Life sciences. 2019;238:116957.
20. Y W, Y L, JY X, ZJ Z, YM X. Let-7d miRNA prevents TGF-β1-induced EMT and renal fibrogenesis through regulation of HMGA2 expression. Biochemical and biophysical research communications. 2016;479(4):676-82.
21. N F, SP C, H OD, F M, C G, DP B, et al. CCN2/CTGF increases expression of miR-302 microRNAs, which target the TGFβ type II receptor with implications for nephropathic cell phenotypes. Journal of cell science. 2012;125:5621-9.
22. CH W, G W, Q C, XC G, F T, R Z, et al. MicroRNA-330-3p promotes cell invasion and metastasis in non-small cell lung cancer through GRIA3 by activating MAPK/ERK signaling pathway. Journal of hematology & oncology. 2017;10(1):125.
23. K K, T H, N K, T A, A O, A K, et al. Regulation of ITGA3 by the anti-tumor miR-199 family inhibits cancer cell migration and invasion in head and neck cancer. Cancer science. 2017;108(8):1681-92.

24. X Z, SP M, D Y, Y L, YP W, T L, et al. miR-142-3p Suppresses Cell Growth by Targeting CDK4 in Colorectal Cancer. Cellular physiology and biochemistry : international journal of experimental cellular physiology, biochemistry, and pharmacology. 2018;51(4):1969-81.
25. YX Y, H Y, J L, XW X, K H, MY H, et al. Up-regulated microRNA-199b-3p represses the apoptosis of cerebral microvascular endothelial cells in ischemic stroke through down-regulation of MAPK/ERK/EGR1 axis. Cell cycle (Georgetown, Tex). 2019;18(16):1868-81.
26. J G, J G, X P, X G, Z J, S Z, et al. Blockade of miR-142-3p promotes anti-apoptotic and suppressive function by inducing KDM6A-mediated H3K27me3 demethylation in induced regulatory T cells. Cell death & disease. 2019;10(5):332.
27. HW L, SQ K, S K, MM A, F G, JL Z, et al. Absence of miR-146a in Podocytes Increases Risk of Diabetic Glomerulopathy via Up-regulation of ErbB4 and Notch-1. The Journal of biological chemistry. 2017;292(2):732-47.
28. D L, D Z, B T, Y Z, W G, Q K, et al. Exosomes from Human Umbilical Cord Mesenchymal Stem Cells Reduce Damage from Oxidative Stress and the Epithelial-Mesenchymal Transition in Renal Epithelial Cells Exposed to Oxalate and Calcium Oxalate Monohydrate. Stem cells international. 2019;2019:6935806.
29. A C, MA P-M, I R, A L, MJ B, MG dB, et al. The transcription factor snail controls epithelial-mesenchymal transitions by repressing E-cadherin expression. Nature cell biology. 2000;2(2):76-83.
30. Lamouille S, Xu J, Derynck R. Molecular mechanisms of epithelial-mesenchymal transition. Nature Reviews Molecular Cell Biology. 2014;15(3):178-96.
31. FV K, GJ H. Remodeling of Ago2-mRNA interactions upon cellular stress reflects miRNA complementarity and correlates with altered translation rates. Genes & development. 2013;27(14):1624-32.
32. S K, L J, L B, J H, M K, M Z. A quantitative analysis of CLIP methods for identifying binding sites of RNA-binding proteins. Nature methods. 2011;8(7):559-64.
33. S G, A F, M M, F K, M S, M H, et al. Unambiguous identification of miRNA:target site interactions by different types of ligation reactions. Molecular cell. 2014;54(6):1042-54.
34. JH K, A S, SS D, SH L, B G, CH C, et al. UTX and MLL4 coordinately regulate transcriptional programs for cell proliferation and invasiveness in breast cancer cells. Cancer research. 2014;74(6):1705-17.
35. S T, T G, C R, G Ö, J F, D A, et al. The histone demethylase UTX regulates stem cell migration and hematopoiesis. Blood. 2013;121(13):2462-73.
36. T vdB, E K, K C, R R, P P, M A, et al. Hypoxia promotes stem cell phenotypes and poor prognosis through epigenetic regulation of DICER. Nature communications. 2014;5:5203.
37. Z Z, HS Z, Y L, ZG Z, GY D, H L, et al. Loss of TET1 facilitates DLD1 colon cancer cell migration via H3K27me3-mediated down-regulation of E-cadherin. Journal of cellular physiology. 2018;233(2):1359-69.
38. ME G, RD H, S D, FM M, D P, AL B, et al. Serum microRNA profiling to distinguish papillary thyroid cancer from benign thyroid masses. Journal of otolaryngology - head & neck surgery = Le Journal d'oto-rhino-laryngologie et de chirurgie cervico-faciale. 2015;44:33.
39. X W, J G, B Z, J X, G Z, Y C. Identification of prognostic markers for hepatocellular carcinoma based on miRNA expression profiles. Life sciences. 2019;232:116596.
40. T S, H Y, M Y, K M, S S, R M, et al. Regulation of ITGA3 by the dual-stranded microRNA-199 family as a potential prognostic marker in bladder cancer. British journal of cancer. 2017;116(8):1077-87.
41. G W, G Y, R Z, G X, L Z, W W, et al. Altered microRNA Expression Profiles of Extracellular Vesicles in Nasal Mucus From Patients With Allergic Rhinitis. Allergy, asthma & immunology research. 2015;7(5):449-57.
42. S D, D G, JI T, D S, G F, V P, et al. Circulating MicroRNAs as Novel Biomarkers of Stenosis Progression in Asymptomatic Carotid Stenosis. Stroke. 2017;48(1):10-6.

Supplementary Figure Legends

Supplementary Figure1. The analyzed results from GEO Datasets.

(A) The expression profile of has-miR-199a-3p/ has-miR-199b-3p in healthy person and patients with diabetic nephropathy from dataset GSE51674 in GEO DataSets. (B) The logFC of miRNA expression analyzed in patients with diabetic nephropathy from dataset GSE51674 compared with healthy person.

Supplementary Figure2. The mRNA expression profile of KDM6A, TGFβ and E-cadherin with the change miR-199b-3p expression.

(A) Relative expression level of miR-199b-3p and KDM6A in HK-2 stable cell line overexpressing mi-NC (HK2-miNC) or miR-199b-3p (HK2-miRNA) cultured in high glucose (HG; 30mM) for 72h. n=3. (B) Relative expression level of TGFβ and E-cadherin in HK-2 stable cell line overexpressing mi-NC or miR-199b-3p cultured in HG for 72h. n=3. (C) Relative expression level of miR-199b-3p and KDM6A in HK2-miRNA cell line with negative control siRNA (inhibitor NC) or miR-199b-3p silence RNA (inhibitor) cultured in HG for 72h. n=3. (D) Relative expression level of TGFβ and E-cadherin in HK2-miRNA cell line with inhibitor NC or inhibitor cultured in HG for 72h. n=3. Mean ± standard error of the mean values are presented. *P < 0.05, **P < 0.01, ***P < 0.005, Student's t test.

Supplementary Figure3. The mRNA expression of KDM6A, TGFβ and E-cadherin in miR-199b-3p knockout mice.

(A) Relative expression level of miR-199b-3p in kidney tissue from different mice. C57BL/Ks mice (WT), miR-199b-3p knockout C57BL/Ks mice (miR-199b3p$^{-/-}$). n=3. (B) Relative expression level of TGFβ, E-cadherin, KDM6A in kidney tissue from different mice with different treatment at 8 weeks after the onset of diabetes. C57BL/Ks mice without any treatment (WT-NC), C57BL/Ks mice treated with STZ (WT-STZ), miR-199b-3p knockout C57BL/Ks mice without any treatment (miR-199b3p$^{-/-}$-NC), miR-199b-3p knockout C57BL/Ks mice treated with STZ (miR-199b3p$^{-/-}$-STZ). n=3. Mean ± standard error of the mean values are presented. **P < 0.01, ***P < 0.005, Student's t test.

Figures

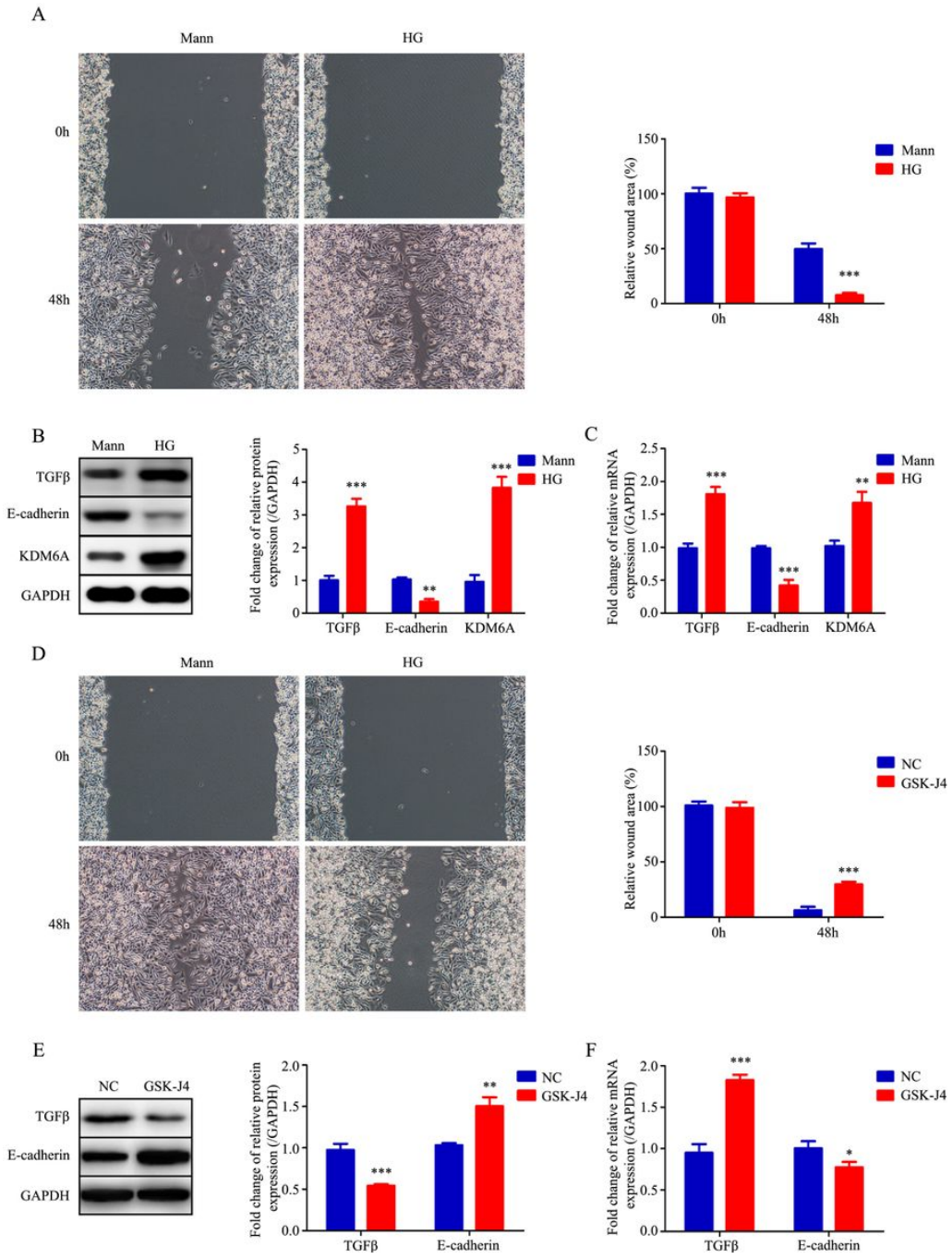

Figure 1

The promotive role of KDM6A in regulating EMT in HK-2 cells. (A) Representative images of migration and graphs of wound area quantification in HK-2 cells cultured in high glucose (HG; 30mM) or high mannitol (Mann; 5mM glucose plus 25mM mannitol) at 0h and 48h. n=10. (B) Western bolt analysis of TGFβ, E-cadherin, KDM6A in HK-2 cells cultured in HG or Mann for 72h. n=3. (C) Relative expression level of TGFβ, E-cadherin and KDM6A by qPCR in HK-2 cells cultured in HG or Mann for 72h. n=3. (D) Representative images of migration and graphs of wound area quantification in HK-2 cells cultured in HG treatment with GSK-J4 (40μM) or equivoluminal ddH2O (NC) at 0h and 48h. n=10. (E) Western bolt analysis of TGFβ, E-cadherin in HK-2 cells cultured in HG treatment with GSK-J4 or ddH2O for 72h. n=3. (F) Expression level of TGFβ, E-cadherin by qPCR in HK-2 cells cultured in HG treatment with GSK-J4 or ddH2O for 72h. n=3. Mean ± standard error of the mean values are presented. *P < 0.05, **P < 0.01, ***P < 0.005, Student's t test.

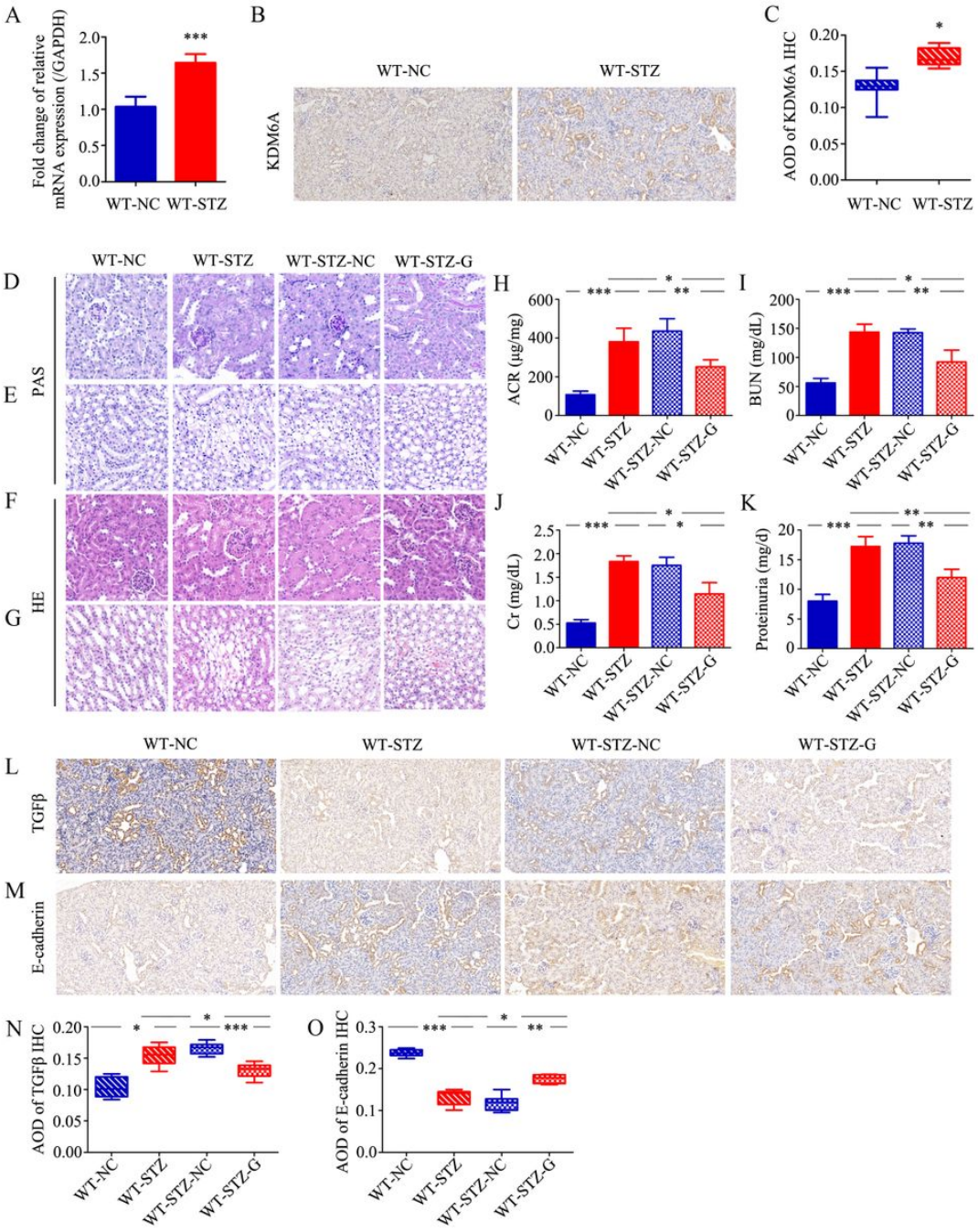

Figure 2

The pivotal role of KDM6A in the progression of kidney injury in DN. (A) Relative expression level of KDM6A by qPCR in kidney tissue from C57BL/6 mice (WT-NC) and STZ-induced mice (WT-STZ) (at 8 weeks after the onset of diabetes). n=3. (B) Representative images of KDM6A immunohistochemical staining in kidney of WT-NC and WT-STZ. Scale bar, 50 μm. (C) Graphs showing quantification (AOD=IOD/Area) of KDM6A immunohistochemical staining results in B. n=10. (D-G) Representative images of PAS staining and HE staining of kidney from different treated C57BL/6 mice. STZ-induced C57BL/6 mice treated without (WT-STZ-NC) or with GSK-J4 (WT-STZ-G). Scale bar, 20 μm. (H-I) Graphs showing the results of ACR, BUN, Cr, proteinuria in different treated mice at 8 weeks after the onset of diabetes. n=6. (L-M) Representative images of TGFβ and E-cadherin immunohistochemical staining in kidney of different treated mice. Scale bar, 50 μm. (N-O) Graphs showing quantification (AOD=IOD/Area) of TGFβ and E-cadherin immunohistochemical staining results in L-M respectively. n=10. Mean ± standard error of the mean values are presented. *P < 0.05, **P < 0.01, ***P < 0.005, Student's t test.

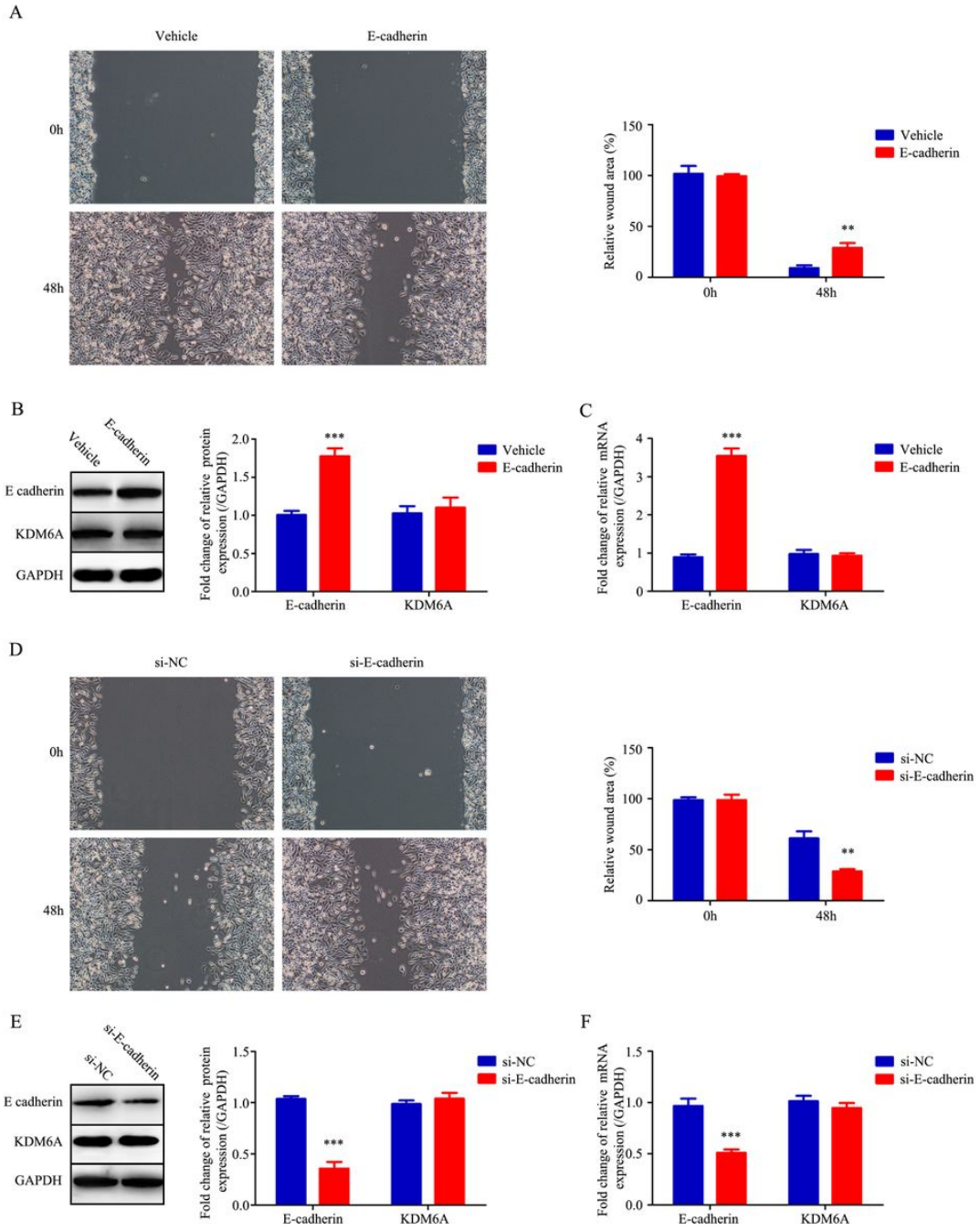

Figure 3

E-cadherin is a downstream target of KDM6A. (A) Representative images of migration and graphs of wound area quantification in HK-2 stable cell line transfected with vehicle including E-cadherin (HK2-E-cadherin) or not (HK2-vehicle) and cultured in high glucose (HG; 30mM) at 0h and 48h. n=10. (B) Western bolt analysis of E-cadherin, KDM6A in HK-2 stable cell line with or without E-cadherin overexpression cultured in HG for 72h. n=3. (C) Relative expression level of E-cadherin, KDM6A by qPCR in HK-2 stable cell line with or without E-cadherin overexpression (vehicle and E-cadherin) cultured in HG for 72h. n=3. (D) Representative images of migration and graphs of wound area quantification in HK2-E-cadherin cell line with or without E-cadherin siRNA (si-NC and si-E-cadherin) cultured in high mannitol (Mann; 5mM glucose plus 25mM mannitol) at 0h and 48h. n=10. (E) Western bolt analysis of E-cadherin, KDM6A in HK2-E-cadherin cells with or without E-cadherin siRNA cultured in Mann for 72h. n=3. (H) Relative expression level of E-cadherin and KDM6A by qPCR in HK2-E-cadherin cells with or without E-cadherin siRNA cultured in Mann for 72h. n=3. Mean ± standard error of the mean values are presented. **P < 0.01, ***P < 0.005, Student's t test.

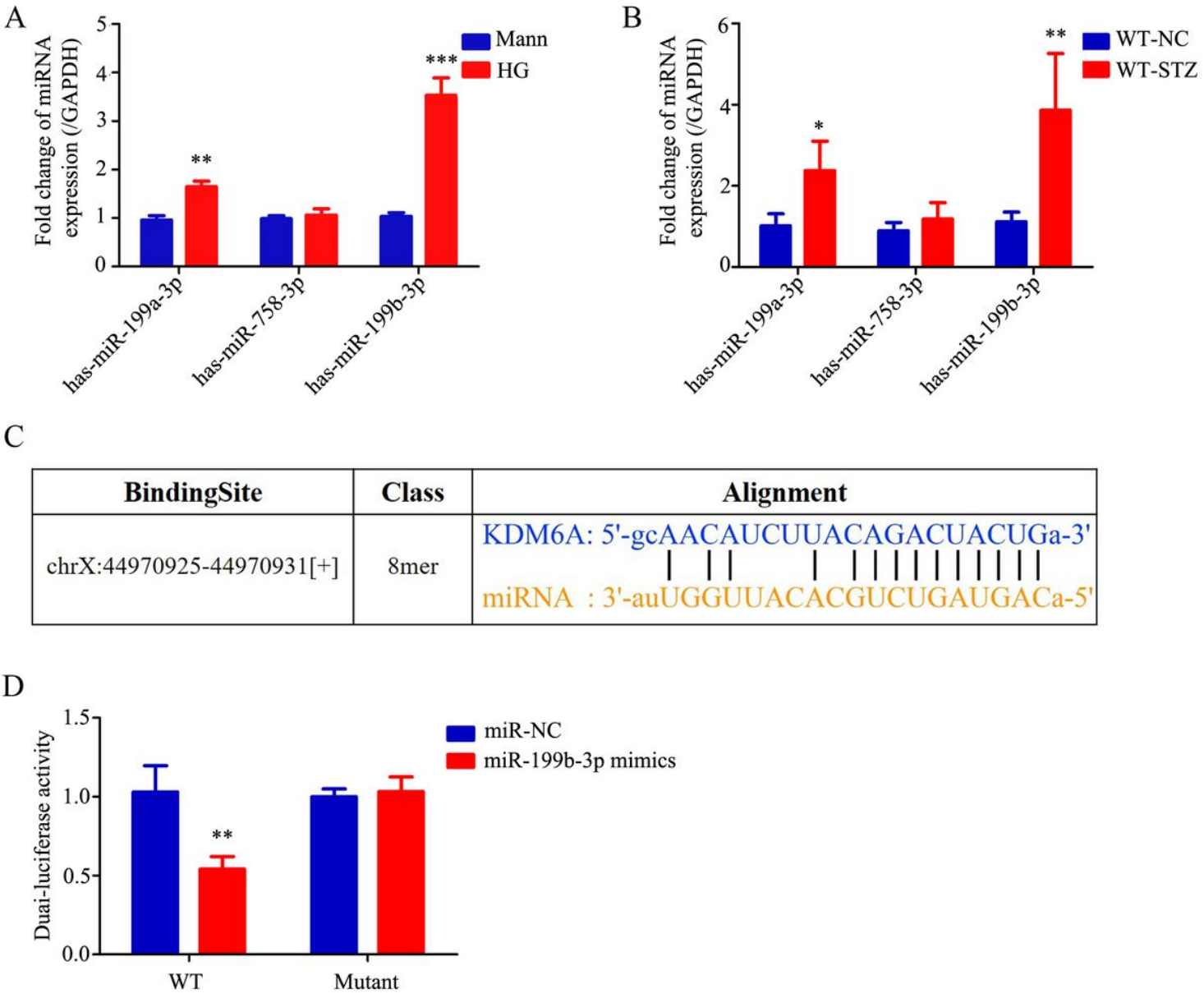

Figure 4

Target prediction and Dual luciferase assay between miRNAs and KDM6A. (A) Relative expression level of miRNAs by qPCR in HK-2 cells cultured in high glucose (HG; 30mM) or high mannitol (Mann; 5mM glucose plus 25mM mannitol) for 72h. n=3. (B) Relative expression level of miRNAs by qPCR in C57BL/Ks mice (WT-NC) and STZ-induced mice (WT-STZ) (at 8 weeks after the onset of diabetes). n=3. (C) Schematic diagram of target prediction between KDM6A and miR-199b-3p. (D) Regulation of miR-199b-3p on 3'-UTR of KDM6A in HEK293T cells by luciferase reporter assay. n=3. Mean ± standard error of the mean values are presented. *P < 0.05, **P < 0.01, ***P < 0.005, Student's t test.

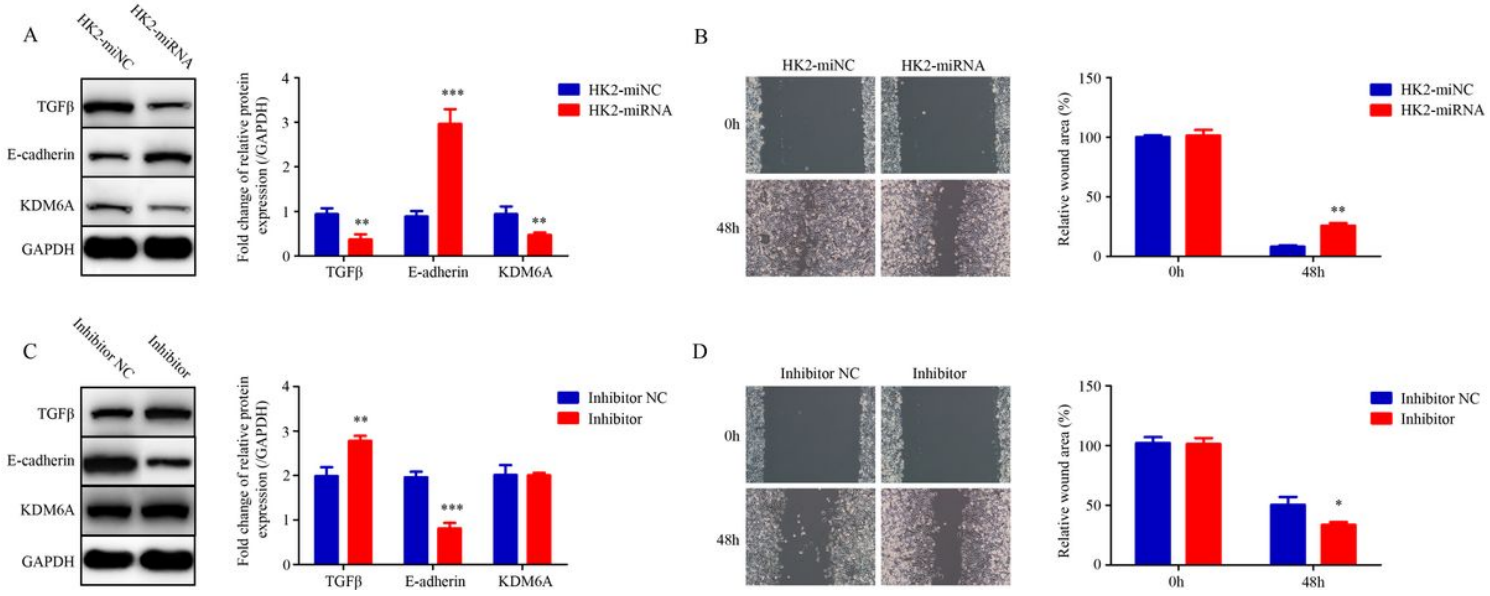

Figure 5

MiR-199b-3p prevent the epithelial-mesenchymal transition of HG-induced HK-2 cells through targeting KDM6A. (A) Western bolt analysis of TGFβ, E-cadherin, KDM6A in HK-2 stable cell line transfected with mi-NC (HK2-miNC) or miR-199b-3p (HK2-miRNA) cultured in high glucose (HG; 30mM) for 72h. n=3. (B) Representative images of migration and graphs of wound area quantification in HK-2 stable cell line with mi-NC or miR-199b-3p cultured in HG at 0h and 48h. n=10. (C) Western bolt analysis of TGFβ, E-cadherin, KDM6A in HK2-miRNA stable cell line with inhibitor NC or inhibitor cultured in HG for 72h. n=3. (D) Representative images of migration and graphs of wound area quantification in HK2-miRNA stable cell line with negative control inhibitor (inhibitor NC) or miR-199b-3p inhibitor (inhibitor) cultured in HG for 72h. n=10. Mean ± standard error of the mean values are presented. *P < 0.05, **P < 0.01, ***P < 0.005, Student's t test.

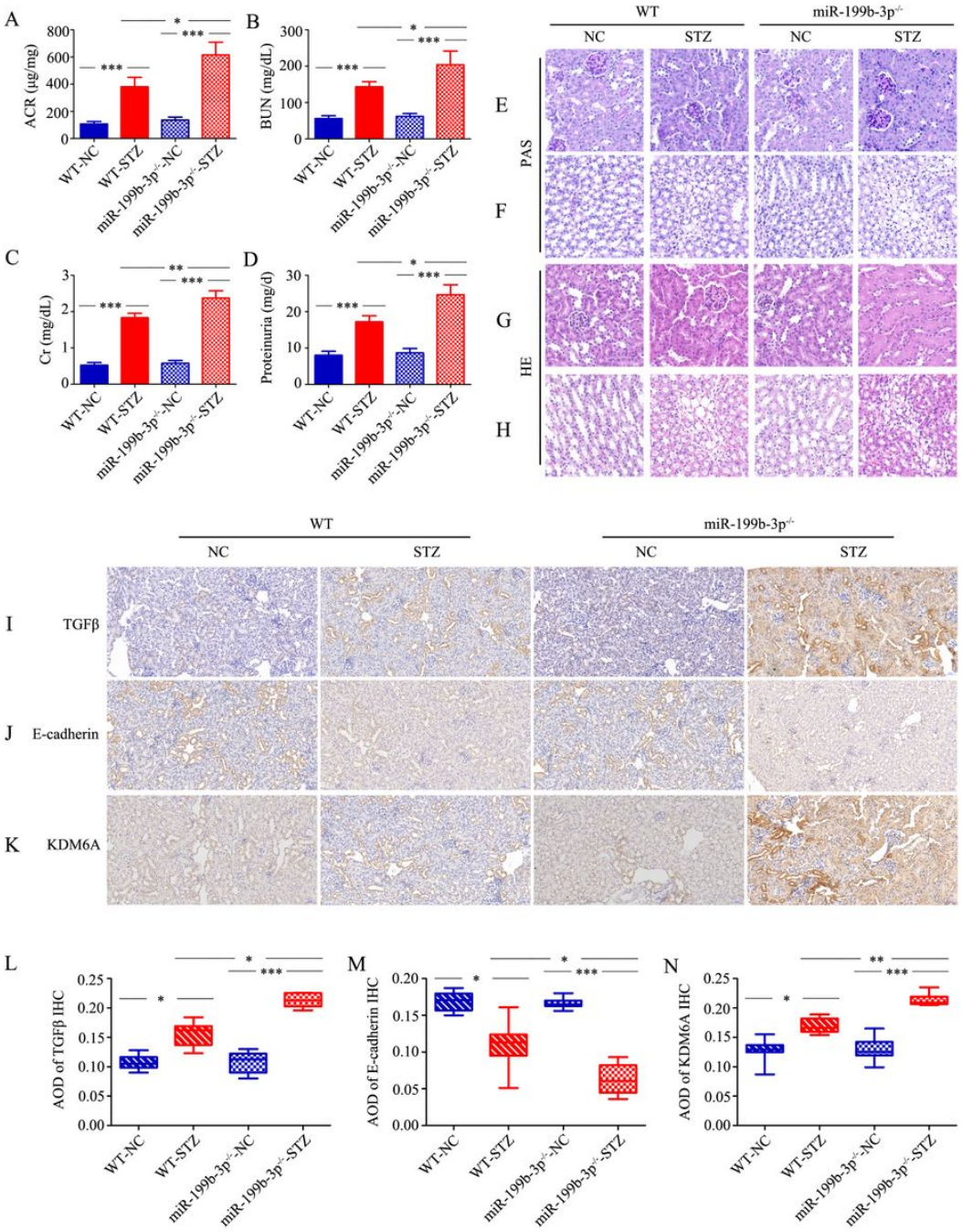

Figure 6

Knockout of miR-199b-3p aggravated renal dysfunction in mice. (A-D) Graphs showing the results of ACR, BUN, Cr, proteinuria in different treated mice at 8 weeks after the onset of diabetes. C57BL/6 mice without any treatment (WT-NC), C57BL/6 mice treated with STZ (WT-STZ), miR-199b-3p knockout C57BL/6 mice without any treatment (miR-199b3p-/–NC), miR-199b-3p knockout C57BL/6 mice treated with STZ (miR-199b3p-/–STZ). n=6. (E-H) Representative images of PAS staining and HE staining of kidney from different mice with different treatment. Scale bar, 20 μm. (I-K) Representative images of TGFβ, E-cadherin, KDM6A immunohistochemical staining in kidney of different mice with different treatment. Scale bar, 50 μm. (L-N) Graphs showing quantification (AOD=IOD/Area) of TGFβ, E-cadherin, KDM6A immunohistochemical staining results in I-K respectively. n=10. Mean ± standard error of the mean values are presented. *P < 0.05, **P < 0.01, ***P < 0.005, Student's t test.

Supplementary Files

This is a list of supplementary files associated with this preprint. Click to download.

- FigureS2.jpg
- FigureS3.jpg
- FigureS1.jpg
- TableS2.docx
- TableS1.docx